

Supplementary information

HIV-1 Treatment Timing Shapes the Human Intestinal Memory B-Cell Repertoire to Commensal Bacteria

Cyril Planchais¹, Luis M. Molinos-Albert^{1,2}, Pierre Rosenbaum¹, Thierry Hieu¹, Alexia Kanyavuz³, Dominique Clermont⁴, Thierry Prazuck⁵, Laurent Lefrou⁶, Jordan D. Dimitrov³, Sophie Hüe⁷, Laurent Hocqueloux⁵, Hugo Mouquet^{1,8}

¹Humoral Immunology Unit, Institut Pasteur, Université Paris Cité, INSERM U1222, F-75015 Paris, France

²Current address: ISGlobal, Hospital Clínic-Universitat de Barcelona, 08036 Barcelona, Spain

³Centre de Recherche des Cordeliers, INSERM, Sorbonne Université, Université de Paris, 75006 Paris, France

⁴Collection of the Institut Pasteur, Institut Pasteur, Université Paris Cité, 75015 Paris, France

⁵Service des Maladies Infectieuses et Tropicales, CHR d'Orléans-La Source, 45067 Orléans, France

⁶Service d'Hépatogastro-entérologie, CHR d'Orléans-La Source, 45067 Orléans, France

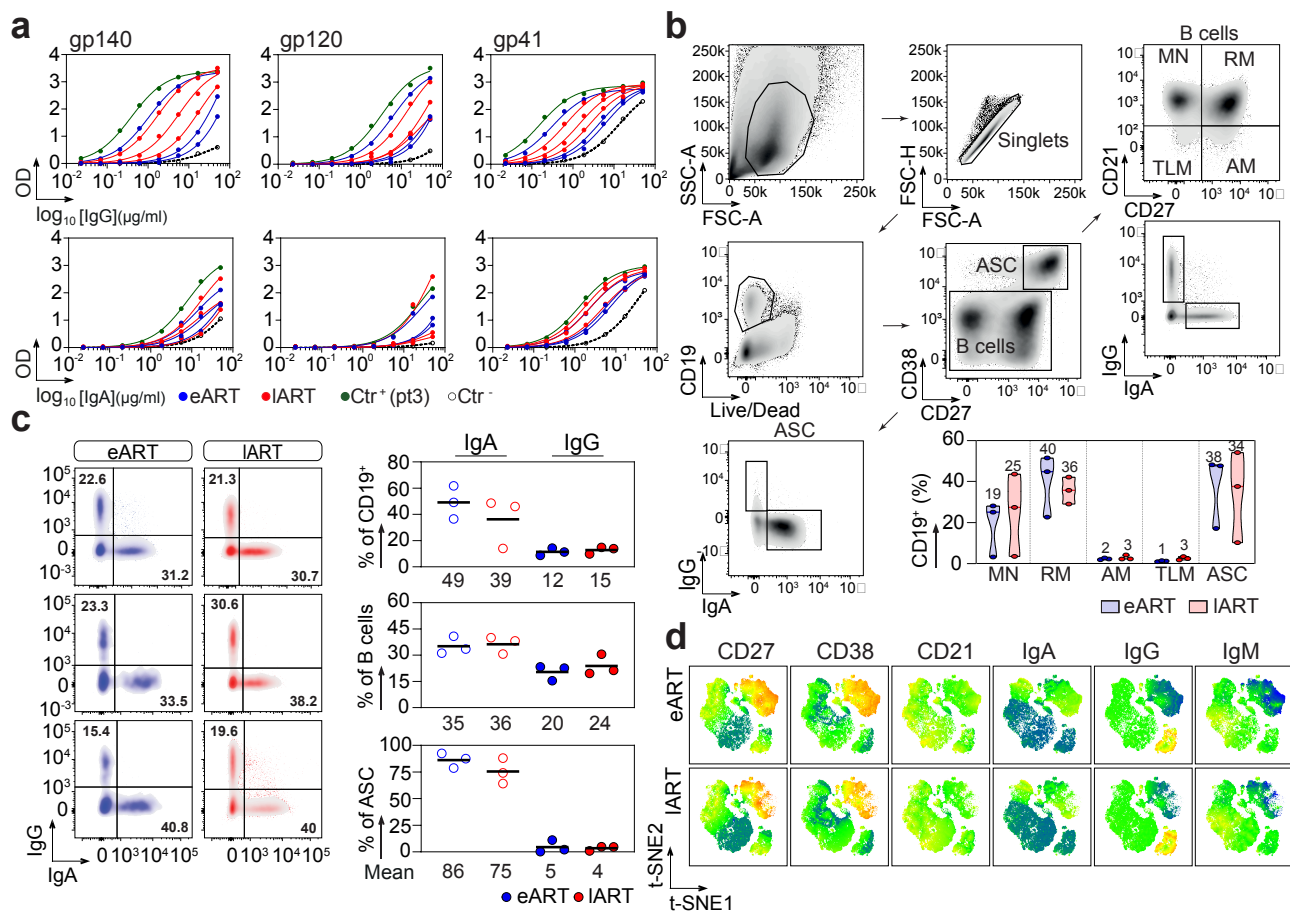
⁷INSERM U955 - Équipe 16, Université Paris-Est Créteil, Faculté de Médecine, 94000 Créteil, France

Supplementary tables 1 and 2

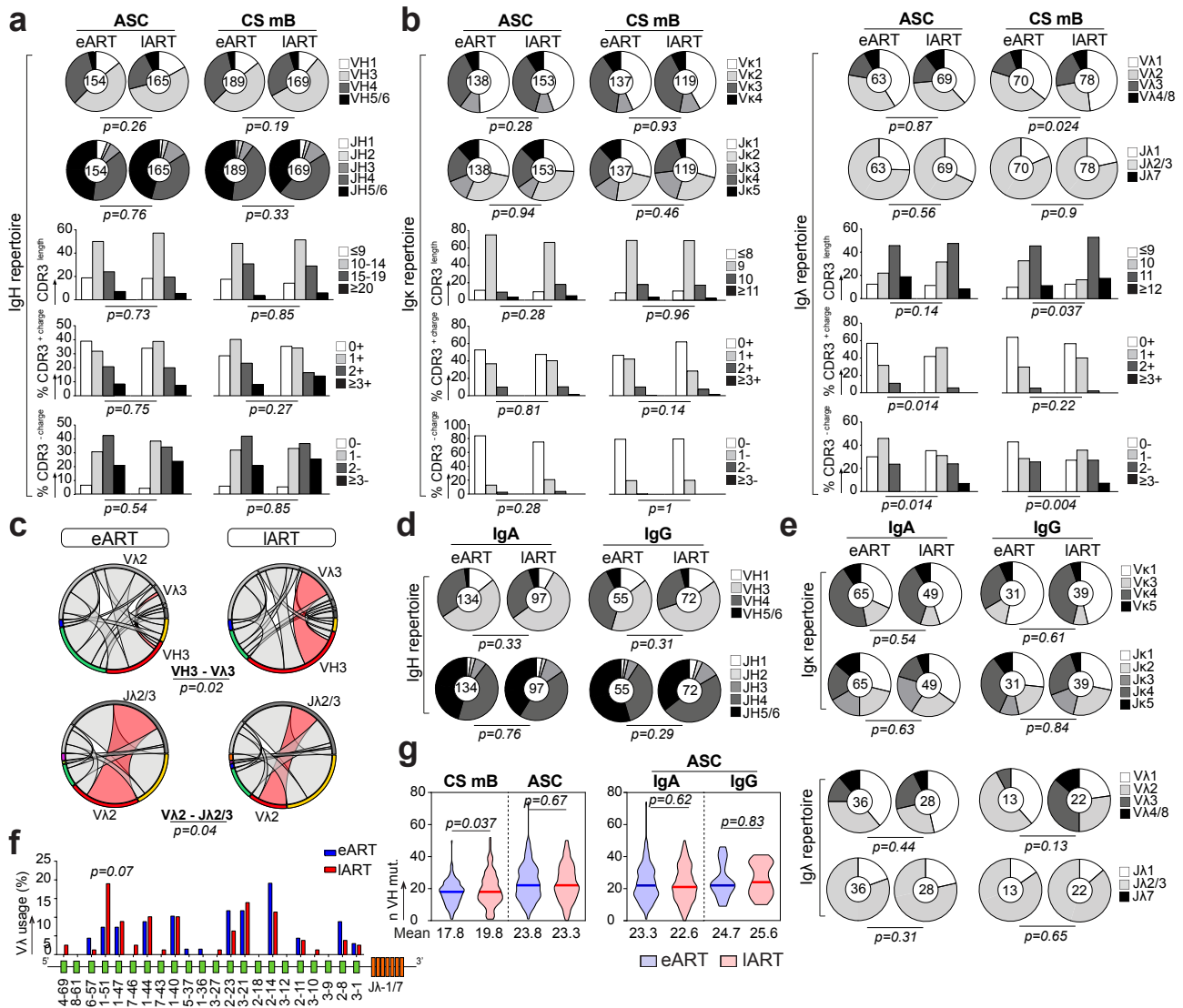
Supplementary figures 1 - 5

Supplementary table 1. Clinical and immunovirological characteristics of eART and IART donors

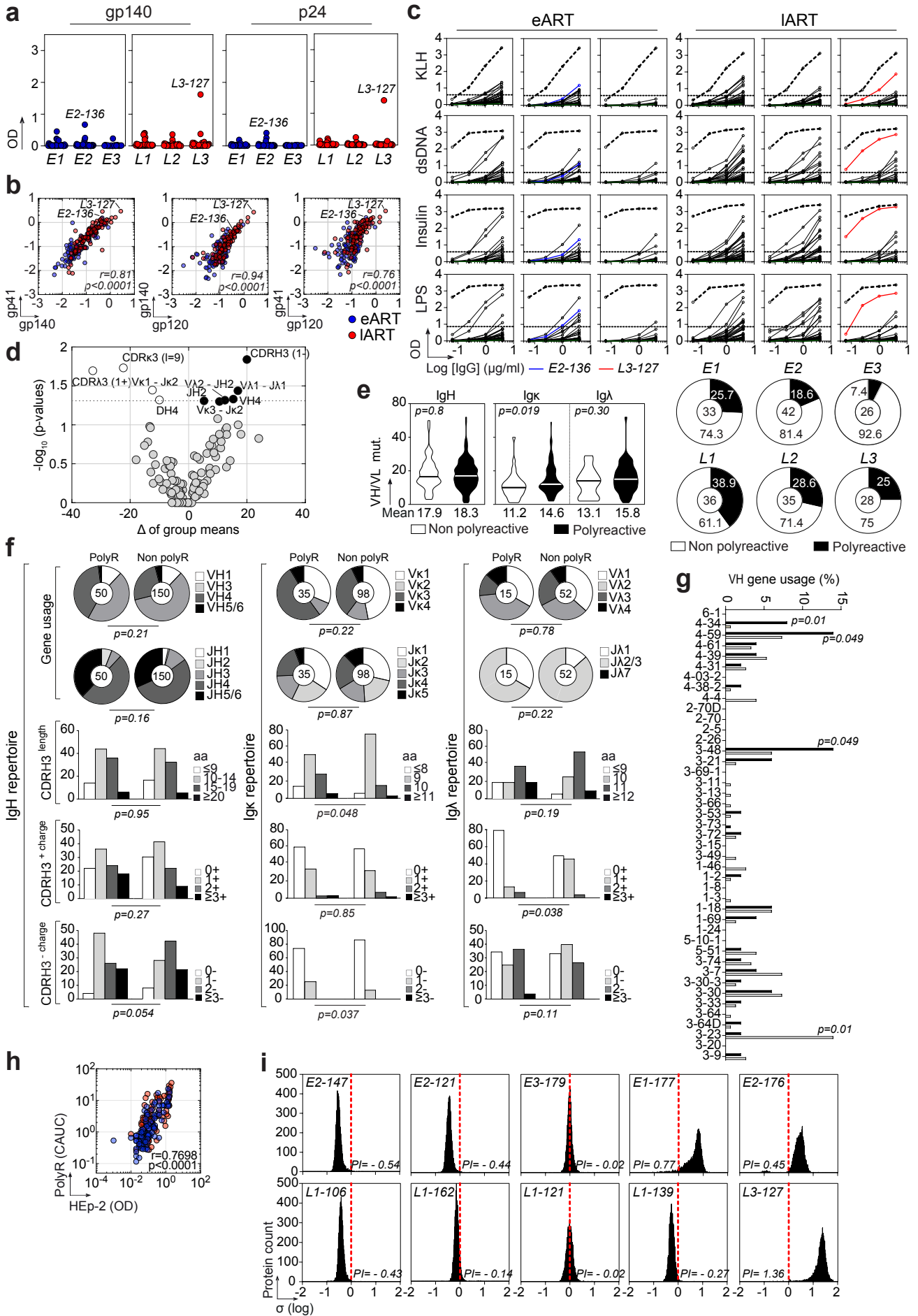
	#	Gender	Age at inclusion (years)	Duration with HIV infection (years)	Time on cART (years)	ART initiation (estimated day post-HIV diagnosis)	Fiebig stage at the start of ART	Duration with PVL<50 copies/ml (years)	nadir CD4 / mm ³	CD4 ⁺ T cells (%)	CD8 ⁺ T cells (%)	CD4 ⁺ T cells (cells/mm ³)	CD8 ⁺ T cells (cells/mm ³)	CD4 / CD8 ratio
eART	E1	F	36	3.2	3.2	10	III	3.1	854	49.8	35.1	1768.4	1246	1.4
	E2	M	65	7.5	7.5	7	IV	6.9	369.3	40.4	23.2	833	478	1.7
	E3	F	48	3.5	3.5	8	V	2.9	374.6	56	25	772.8	345	2.2
	E4	F	36	3.4	3.4	26	V	2.9	521.4	49	25	1353	690	2.0
	E5	M	53	5.1	5.1	2	IV	4.7	1253	54	19	1863	647	2.9
	E6	F	41	19.4	19.4	0	IV	1.5	524.3	43	43	864	868	1.0
	E7	M	38	1.4	1.4	7	III	1.3	608.8	42	36	1125	954	1.2
	E8	M	55	11.6	11.6	3	III	4.0	815	41	22	1060	579	1.8
	E9	M	69	5.7	5.7	1	V	4.9	401.5	38.6	36.4	475.6	449	1.1
	E10	M	41	6.1	6.1	21	V	5.9	570	44	21	947	462	2.0
	E11	M	31	9.9	9.9	6	V	9.2	405	34.2	46.4	731.9	993	0.7
	E12	M	70	10.6	10.5	27	V	0.9	500.1	41	41	872	885	1.0
	E13	M	46	11.5	11.5	20	V	3.9	368.5	43	26	668	403	1.7
	E14	M	44	8.4	8.3	15	V	7.4	450	41	42	1051	1070	1.0
	E15	M	53	10.6	10.6	26	V	9.2	664	43	42	937	913	1.0
	E16	F	51	17.9	17.7	76	V	0.3	496.3	51.4	27.7	1459.2	787	1.9
	E17	M	63	2.1	2.1	17	V	1.2	249	36	26	519	373	1.4
	E18	M	47	3.2	3.2	16	IV	2.7	355.7	39	35	538	483	1.1
	E19	M	40	3.5	3.4	18	IV	2.0	262.8	38	37	831	818	1.0
	E20	M	63	12.9	12.8	35	V	3.8	445.6	43	34	676	534	1.3
	E21	M	55	2.4	2.3	18	IV	1.5	214.9	44	33	461	342	1.3
	E22	M	35	3.6	3.6	6	III	3.2	582.8	40	29	1148	832	1.4
	E23	M	43	9.7	9.6	20	IV	8.0	723.4	50	29	1094	646	1.7
	E24	M	51	14.5	14.4	15	V	8.8	329	37	40	952	1050	0.9
	E25	F	79	19.5	19.3	54	V	7.5	407.9	48	20	1067	452	2.4
	E26	M	40	3.2	3.2	11	IV	2.8	627.4	47	30	1374	878	1.6
	E27	M	68	10.5	10.5	12	IV	8.7	390.6	24	32	611	806	0.8
	E28	M	32	3.2	3.2	9	IV	3.1	442.5	50	30	1004	597	1.7
	E29	M	57	3.8	3.7	40	V	3.6	732	38	22	836	470	1.8
	E30	M	45	13.1	13.0	10	V	3.5	320	39.9	48	551	663	0.8
	E31	M	53	16.7	16.7	9	V	16.0	402.1	33	28	861	731	1.2
	E32	M	48	23.0	22.8	52	V	11.2	320.6	36	40	527	587	0.9
	E33	M	56	9.8	9.7	8	IV	8.8	392	30	40	572	750	0.8
	E34	M	49	2.2	2.2	18	V	1.9	283.1	40	42	708	742	1.0
E35	M	28	1.7	1.7	0	V	1.3	334.4	37.7	38.4	941.4	960	1.0	
E36	M	36	2.5	2.5	3	V	2.2	589.4	33	37	1101	1216	0.9	
E37	M	35	3.0	3.0	5	II	1.7	293.6	25	31	493	612	0.8	
E38	F	57	10.0	9.9	22	V	9.7	835	52	34	2309	1501	1.5	
IART	L1	M	58	11.6	8.2	1242	VI	4.4	205.2	36.2	42.7	925.6	1092	0.8
	L2	F	69	21.5	21.2	105	VI	10.3	284.8	36	33	792	726	1.1
	L3	M	50	22.4	21.2	454	VI	3.9	63.9	29	38	765.6	1003	0.8
	L4	F	80	19.1	19.0	21	VI	10.3	6.3	34.2	38.8	221	251	0.9
	L5	M	52	22.8	9.9	1887	VI	6.7	125	19.5	32	377	531	0.7
	L6	F	34	13.0	12.9	28	VI	3.7	227.8	35.7	32.9	479	442	1.1
	L7	F	54	12.8	12.8	5	VI	4.8	231	30.3	20.4	1564.1	1052	1.5
	L8	F	53	5.3	3.2	775	VI	1.5	341	46	32.2	915.4	640	1.4
	L9	F	52	8.6	5.3	1217	VI	5.0	307	43.2	24.5	709.3	403	1.8
	L10	M	43	10.7	10.1	232	VI	6.3	306	49	28.9	1120	665	1.7
	L11	F	38	10.8	10.7	8	VI	0.0	251.1	35.7	28.4	643	512	1.3
	L12	M	72	10.6	10.5	51	VI	6.5	149.1	30.5	26.6	597.2	521	1.1
	L13	F	57	3.5	3.4	12	VI	3.1	343	40.1	50	978	1219	0.8
	L14	M	46	19.5	17.7	660	VI	6.6	287.3	42.3	38	933	840	1.1
	L15	M	50	0.3	0.2	29	VI	0.0	29	12.7	78.3	59.2	365	0.2
	L16	M	50	14.5	14.5	0	VI	2.2	169.2	23.5	35.2	475	713	0.7
	L17	F	69	10.8	9.2	567	VI	8.9	154	37.2	41.9	762	866	0.9
	L18	M	73	9.1	9.1	4	VI	8.5	164	32.3	26.7	501.6	415	1.2
	L19	M	38	0.3	0.2	26	VI	0.0	69	11.7	61.8	88	465	0.2
	L20	M	52	16.1	16.0	31	VI	8.2	76	27.3	52.9	494	957	0.5
	L21	M	69	31.6	11.6	7300	VI	0.5	147	16.5	66.2	269.6	1082	0.2
	L22	M	63	3.1	3.1	28	VI	2.7	616	43	31.6	1127	828	1.4
	L23	M	39	13.1	11.6	548	VI	4.6	479.5	37.2	29.3	702.7	554	1.3
	L24	M	60	16.7	16.7	19	VI	1.0	6	8.8	17.9	446.2	905	0.5
	L25	M	41	2.7	2.2	197	VI	1.8	665	35	34.3	1386	1356	1.0
	L26	F	42	4.9	4.9	0	VI	4.5	398	33.9	51.5	892	1355	0.7
	L27	F	26	25.9	20.0	2148	VI	0.0	11.1	38.9	56.3	26	620	0.0
	L28	F	47	13.9	13.9	17	VI	1.8	290.8	42.6	30.2	759	539	1.4
	L29	F	47	5.6	5.6	18	VI	5.3	167.4	39.6	41.6	379	398	1.0
	L30	F	23	1.6	0.6	376	VI	0.0	505	35.6	35	934.1	918	1.0
	L31	M	64	17.4	17.3	32	VI	1.3	127.7	39.5	43.7	421	465	0.9
	L32	F	57	0.4	0.2	83	VI	0.0	172	13.4	68.3	235	1201	0.2
L33	M	49	4.6	4.6	10	VI	0.5	229	38.9	25.9	1020	679	1.5	
L34	F	27	8.9	6.6	828	VI	0.0	82	16.5	52.2	224	707	0.3	
L35	F	64	13.1	12.9	68	VI	12.6	214.3	28.3	38.6	496	676	0.7	
L36	F	31	5.6	5.6	15	VI	5.0	300.8	31.8	42.2	864.3	1146	0.8	
L37	F	54	20.9	19.8	402	VI	12.5	212.4	29.9	36.3	676.9	821	0.8	
L38	F	45	3.5	3.5	0	VI	2.5	459.3	20.4	47.1	663	773	0.9	
L39	F	33	15.1	3.1	4395	VI	0.0	131	20.4	47.1	688.1	1588	0.4	
L40	M	45	19.7	3.0	6097	VI	2.7	213	37	40.2	464.7	505	0.9	



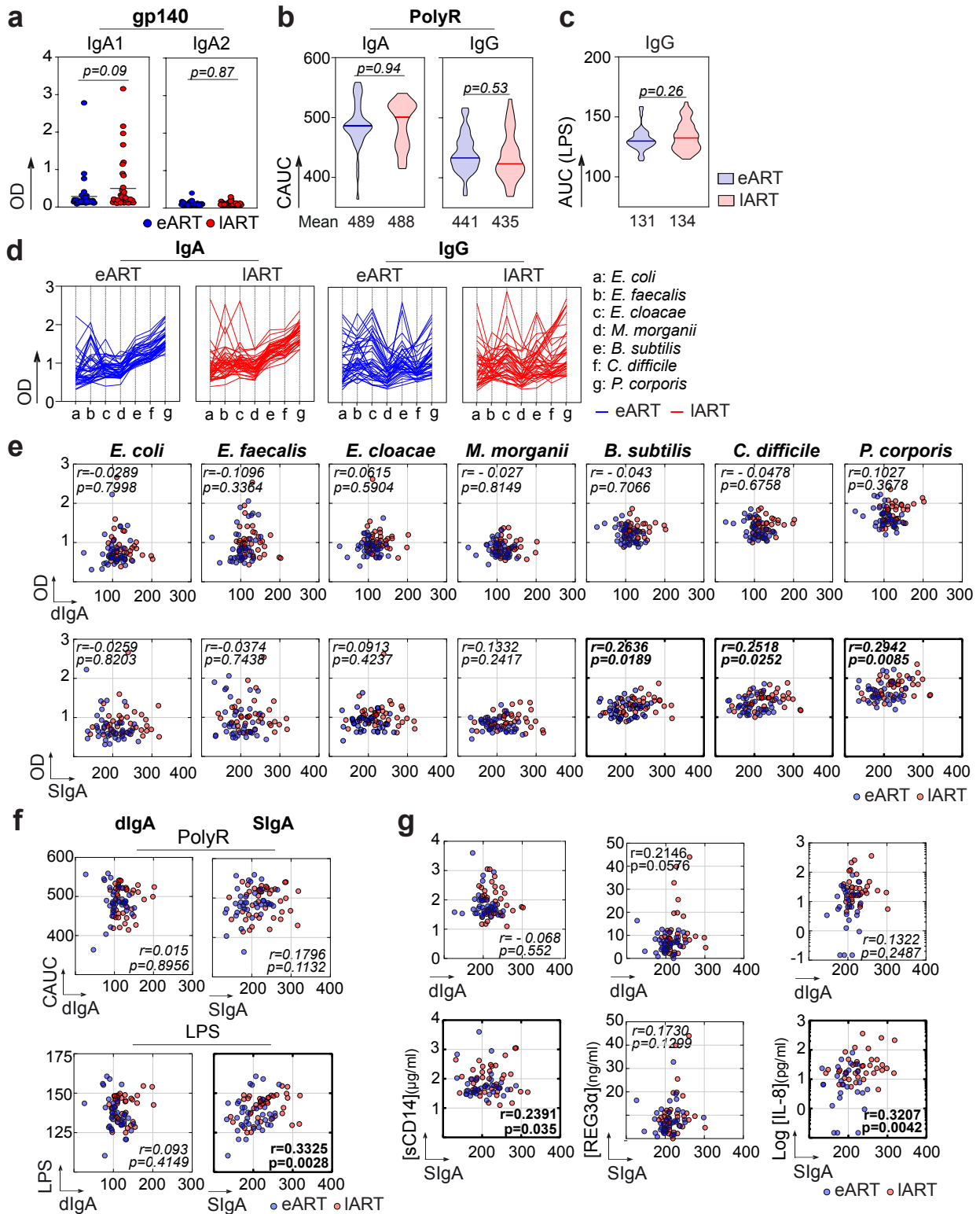
Supplementary Fig. 1 | Intestinal IgA⁺ and IgG⁺ B cells from eART and IART. **a** ELISA graph showing the reactivity of purified serum IgG and IgA antibodies from eART (n=3, blue) and IART (n=3, red) against trimeric gp140-F, gp120, and gp41 proteins. Means \pm SEM of values from two independent experiments (performed in duplicate) are shown. Ctr⁺, positive control (pt3⁸⁶); Ctr⁻, non-HIV-1 negative control. **b** Cytograms (top) and dot plots (bottom) showing the flow cytometry gating strategy and frequency comparison for mature naïve (MN), resting memory (RM), activated memory (AM), tissue-like memory (TLM) B cells and antibody-secreting cells (ASC) between eART (n=3) and IART (n=3). **c** Cytograms (left) showing the flow cytometry gating strategy and dot plots (right) comparing the IgA⁺ and IgG⁺ B-cell frequencies between eART (n=3) and IART (n=3). The average frequency of IgA⁺ and IgG⁺ cells among total CD19⁺ cells, B cells and ASC is indicated below each dot plot. **d** t-SNE-based analysis of intestinal CD19⁺ cells from eART and IART (n=3; 2 x 10⁵ cells per group). Two-dimensional t-SNE plots depict the expression levels (color-coded: blue (low) to red (high)) of surface IgA, IgG, IgM, CD21, CD38 and CD27 markers. Source data are provided as a Source Data file.



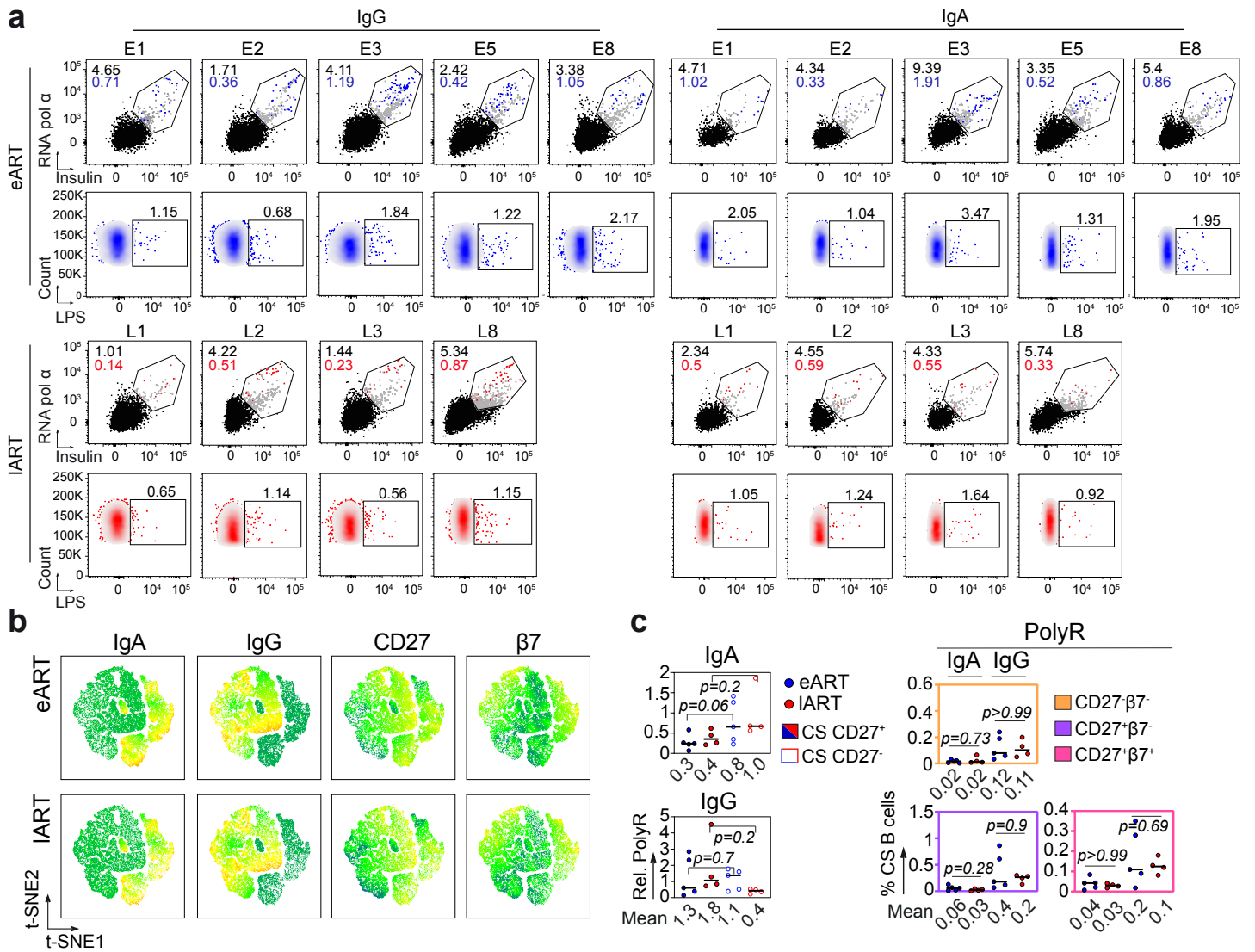
Supplementary Fig. 2 | Immunoglobulin gene features of intestinal IgA⁺ and IgG⁺ B cells. **a** IgH gene features. Pie charts (top) comparing the distribution of V and J gene usage in mucosal B cells (class-switched memory B cells [CS mB] and ASC) between eART and IART (n=3 *per* group). The number of antibody sequences analyzed is indicated in the center of each pie chart. Groups were compared using 2 × 5 Fisher's Exact test. Bar graphs (bottom) showing the distribution of CDR3 lengths, positive and negative charge numbers in intestinal B-cell antibodies from eART and IART. **b** Same as in (a) but for Igk (left) and Igλ (right) gene features. **c** Circos plots generated with immunoglobulin gene data of intestinal memory B cells using "circlize" R package (v0.3.1) comparing between eART and IART, VH/Vλ and Vλ/Jλ association and rearrangement frequencies, respectively. Groups were compared using 2 × 5 Fisher's Exact test. **d** Pie charts comparing the distribution of V and J gene usage in IgA⁺ and IgG⁺ memory B cells between eART and IART. **e** Same as in (d) but for Igk (top) and Igλ (bottom) genes. **f** Bar graphs comparing the Vλ gene distribution in single intestinal memory B cells between eART and IART. Groups were compared using 2 × 2 Fisher's Exact test. **g** Violin plots comparing the number VH gene mutations in gut memory B cells and ASC between eART and IART. The average number of mutations is indicated below each violin plot. Numbers of somatic mutation (n VH mut.) were compared using two-tailed unpaired student t-test with Welch's correction. Source data are provided as a Source Data file.



Supplementary Fig. 3 | Polyreactivity of intestinal memory B cells. **a** Dot plots comparing the reactivity of mucosal antibodies (n=200) from eART and IART (n=3 *per* group) against HIV-1 Env proteins (gp140-F, gp120 and gp41) determined in triplicate using classical ELISA. **b** Correlation plots (bottom; \log_{10} OD binding values) comparing the reactivity of mucosal antibodies (n=200) from eART (blue) and IART (red) against HIV-1 Env proteins (gp140-F, gp120 and gp41) using polyreactive ELISA. Bivariate correlations were estimated with the two-tailed Pearson correlation test. **c** ELISA graphs comparing the polyreactivity of the mucosal antibodies cloned from eART and IART donors (n=3 *per* group) against KLH, dsDNA, insulin and LPS. mGO53 (green line) and ED38 (dotted line) are negative and positive control antibodies, respectively. Horizontal lines show cutoff for positive reactivity. Pie charts (below) present the frequency of polyreactive (black) and non-polyreactive (white) intestinal memory B-cell antibodies *per* individual. The number of tested antibodies is indicated in the pie chart center. Means \pm SEM of values from two independent experiments (performed with duplicate) are shown. **d** Volcano plots comparing the gene features (n=260 parameters) of polyreactive and non-polyreactive intestinal memory B-cell antibodies. The y axis indicates the statistics expressed as $-\log_{10}$ (p values) and the x axis represents the differences between the group means for each parameter. Dashed lines indicate the significance cut off $p < 0.05$. **e** Violin plots comparing the number of VH, V κ and V λ gene mutations between poly- and non-polyreactive mucosal antibodies. The average number of somatic mutations is indicated below each violin plot. Numbers of mutation were compared between groups using unpaired student t-test with Welch's correction. **f** IgH, Igk and Igl gene features of polyreactive and non-polyreactive antibodies. Pie charts (top) showing the distribution of VH/VL and JH/JL gene usage in polyreactive and non-polyreactive mucosal memory B-cell antibodies. Bar graphs (bottom) showing the distribution of CDR3 lengths, positive and negative charge numbers in polyreactive and non-polyreactive mucosal memory B-cell antibodies. The number of antibody sequences analyzed is indicated in the center of each pie chart. Groups were compared using 2×5 Fisher's Exact test. **g** Bar graphs comparing the distribution of VH genes expressed by single poly- and non-polyreactive intestinal memory B-cell antibodies. Groups were compared using 2×2 Fisher's Exact test. **h** Correlation plot comparing the levels of antibody polyreactivity (polyR, as cumulative area under the curve [CAUC]) and HEp-2-reactivity determined by ELISA in eART (blue) and IART (red). Bivariate correlation was estimated using the two-tailed Pearson correlation test. **i** Frequency histograms show the \log_{10} protein displacement (σ) of the mean fluorescent intensity (MFI) signals for the selected antibodies (n = 10) compared with non-reactive antibody mGO53. The polyreactivity index (PI) corresponds to the Gaussian mean of all array protein displacements. Source data are provided as a Source Data file.



Supplementary Fig. 4 | Reactivity of serum IgA and IgG antibodies from eART and IART. **a** Dot plots comparing the IgA1 and IgA2 reactivity against HIV-1 gp140-F of purified serum IgA antibodies between eART (n=38) and IART (n=40). Each dot corresponds to the mean of triplicate values. Groups were compared using Student's t-test with Welch's correction. **b** Violin plots comparing the polyreactivity of purified serum IgA and IgG antibodies from eART (n=38) and IART (n=40). Mean values from two independent experiments (performed in duplicate) were used. The y axis indicates the CAUC values for the polyreactivity. CAUC mean is indicated below each violin plot. **c** Violin plots comparing the reactivity of purified IgG antibodies against LPS. Mean values from two independent experiments (performed in duplicate) were used. The y axis indicates the AUC values for the LPS reactivity. AUC mean is indicated below each violin plot. **d** Graphs comparing the reactivity profiles against commensal bacteria of purified serum IgA and IgG antibodies from eART (n=38) and IART (n=40). Means from duplicate values are shown. **e** Correlation plots comparing total serum dIgA and SIgA levels with the IgA reactivity against selected commensal bacteria in eART eART (n=38) and IART (n=40). **f** Correlation plots comparing total serum dIgA and SIgA levels with the IgA poly- and LPS-reactivity in eART and IART. **g** Correlation plots comparing serum dIgA and SIgA levels with the serum concentration of sCD14, REG3α and IL-8. Bivariate correlations were estimated with the two-tailed Pearson correlation test with Welch's correction. Source data are provided as a Source Data file.



Supplementary Fig. 5 | Polyreactive binding of class-switched memory B cells from eART and IART. **a** Flow cytograms showing the gating strategy used to determine the frequency of polyreactive blood IgA⁺ and IgG⁺ B cells from eART (n=5) and IART (n=4). The frequency of antigen-reactive cells is indicated above each gate. Colored values indicate the frequency of B cells reactive with all antigens tested (RNAPol α , LPS and Insulin), which were defined as polyreactive (polyR) B cells. **b** t-SNE-based analysis of blood IgA⁺ and IgG⁺ B cells from eART (n=4) and IART (n=5) (2 x 10⁵ cells per group). Two-dimensional t-SNE plots depict the expression levels (color-coded: blue (low) to red (high)) of IgA, IgG, CD27 and β 7 surface markers. **c** Dot plots comparing the relative polyreactivity (rel. PolyR; calculated as the % of polyR B cells / % of total B cells in the subset) of CD27⁺ (plain circles) or CD27⁻ (open circles) class-switched (CS) B-cell sub-populations between eART (blue) and IART (red) (left). The average value is indicated below each dot plot. Dot plots comparing between eART and IART the distribution of polyreactive cells (PolyR) among the B-cell subsets described in Fig. 5b. The average frequency of cells among the total IgA⁺ and IgG⁺ B cells is indicated below each dot plot. Groups were compared using Student's t-test with Welch's correction. Source data are provided as a Source Data file.